Phenomenological model of the quantum size effect on growth of nanosize towers in Pb/Si(111) and Pb/Cu(111)

2008 J. Phys.: Condens. Matter 20 175219

(http://iopscience.iop.org/0953-8984/20/17/175219)

IOP PUBLISHING JOURNAL OF PHYSICS: CONDENSED MATTER

J. Phys.: Condens. Matter **20** (2008) 175219 (6pp) doi:10.1088/0953-8984/20/17/175219

Phenomenological model of the quantum size effect on growth of nanosize towers in Pb/Si(111) and Pb/Cu(111)

H Ristolainen and I T Koponen

Department of Physical Sciences, University of Helsinki, PO Box 64, FI-00014, Finland

E-mail: heikki.ristolainen@helsinki.fi

Received 24 October 2007, in final form 12 February 2008
Published 7 April 2008
Online at stacks.iop.org/JPhysCM/20/175219

Abstract

In the growth and formation of nanoscaled structures on Pb/Si(111) and Pb/Cu(111), certain heights of the structures have increased stability, which leads to the formation of tower-like structures (nanotowers). Typically, such Pb nanotowers with even numbers of layers up to 8 are found to be stable, as well as towers with odd numbers of layers from 11 onwards. The stability of these preferred heights is due to the electronic structure dependent total energy, the so-called quantum size effect (QSE). We present here a simple phenomenological model describing the QSE on nanostructure growth. The basic model is a modification of the simultaneous multilayer growth model, relating the mass redistribution between different layers to Friedel-type surface energetics in order to capture the QSE. In the model, the structures consisting of even numbers of layers (4, 6, 8) and odd numbers of layers (11 and 13 onwards) are stable, and are shown to have tower-like morphology.

1. Introduction

In quantum dot (QD) growth there are interesting situations where the height selection of certain stable QDs occurs during their growth [1–3]. An extensively studied case is the formation of Pb nanotowers on Si(111) [2–7] or Cu(111) [8–11]. In Si(111) and Cu(111) the Pb nanotowers tend to grow in bilayer growth mode, in which two layers will form simultaneously until the stable heights—typically 6, 8, 10, 11 and 15 (the stability of heights 4, 10 and 13 are somewhat unclear)—are reached. Towers consisting of 5, 9, 12, 14 layers are unstable [2–11]. The origins of the height selection, stability and simultaneous bilayer growth are well understood in terms of confined electronic states in QDs, and the effect of confinement on the total energy of a system can be quite accurately described in terms of the Friedel-oscillations [4, 5, 9, 10, 13, 12]. In Pb/Si and Pb/Cu systems, the differences in total energies of the alternating layers, as inferred from experiments and *ab initio* calculations [3, 5, 6, 10–12], are expected to be only of order 25–50 meV per surface atom.

The knowledge about the effect of electronic structure on energetics and stability forms only the first step towards understanding the growth and formation of height-selected QDs. The growth and decay of nanostructures is often modelled by the so-called step models, where surfaces are treated as step-like geometric structures on which the adatoms move. The step models have been quite successful in explaining the basic features of nanostructure growth and morphological transformations [14–18]. However, it is interesting to try to understand the basic aspects of such phenomena in less complicated terms by relating the evolution of nanostructures more directly to macroscopic mass currents and their dependence on the structure morphology.

In this work, we present a simple phenomenological model, which describes the QSE on nanotower growth through the Friedel model and reproduces the experimentally observed height selection in Pb/Si and Pb/Cu systems. The model is a modification of the so-called 'wedding-cake' models, which treat the surfaces as a stack of concentric layers, focusing on the changes of the total coverages of the layers during the growth [19–23]. The mass redistribution is described in terms of macroscopic mass currents, which depend on film morphology as well as the energetic stability as given by the Friedel model. Therefore, the energetic stability is not a prediction of the model, but rather a built-in feature which defines how the morphology becomes affected by the energetics. Such a model can capture the minimal

set of assumptions needed to understand the interrelation between morphological evolution of nanostructures and the mass redistribution guided by energetics. Because of the simplicity of our model, its results are only qualitative, but they suggest that the underlying processes needed to reproduce the basic generic features of height selection caused by the QSE are quite simple.

2. The phenomenological model

In small systems, the quantum mechanical effects of electron confinement cause clear size dependent variations in the total surface energy, and this so-called quantum size effect (QSE) favours the stability of certain sizes and heights of the structure [2–6, 9, 10, 12]. The energetics originating from the QSE can be modelled with Friedel-type surface energy

$$E_n = A\frac{\cos[2k_F d(n+\Delta n)]}{(n+\Delta n)^\alpha} + B, \qquad (1)$$

which oscillates as a function of the structure height n. The parameters of the Friedel model depend slightly on the method used, or how they are inferred from the experiments. In what follows, we use $k_F = 15.9\ \mathrm{nm}^{-1}$ for the free electron Fermi wavevector, $d = 0.284$ nm for the thickness of a single Pb layer, and $\alpha = 0.938$ to describe the decay of the oscillations with increasing height. The additional parameter $\Delta n = 0.30$ takes into account the fact that the quantum well may be slightly deeper than nd due to the charge spillage effect [5]. The values of these parameters are chosen to agree with the ones given in [5], but also different parametrizations yielding basically similar results are possible [6]. The parameters A and B define the absolute energy scale. In the following $B = 0$ and $A \approx 150$ meV for Pb/Si and 300 meV for Pb/Cu systems are used, so that the minimum energy barrier occurring at $n = 7$ is $\Delta E_7 \approx 20$ meV for Si (cf [5]) and 40 meV for Cu. The temperatures of interest are $T = 150$–250 K and $T = 250$–450 K, for Si and Cu systems, respectively. For convenience we use scaled dimensionless energies $E_n \to E_n/A$ and temperatures $T \to k_B T/A$, with values $A = 150$ meV for Si and 300 meV for Cu.

2.1. The rate equations of growth

The phenomenological model to be constructed here is a 'wedding-cake' model, where the growing nanostructure consists of concentric layers with coverages θ_n, $n = 1, \ldots, N_{\mathrm{top}}$, and where the coverages are scaled with the bottom layer area θ_0 [20]. Following the diffusion corrected simultaneous multilayer (DSCM) growth model proposed by Fu and Wagner [22], we make a simplifying assumption that the evolution of the morphology can be described in terms of mass currents J_n feeding the growth, and in terms of interlayer mass transfer rates γ_n governing the mass redistribution between the adjacent atomic layers. The feeding current J_n (see section 2.3) comes from the wetting layer of adatoms, which is pre-deposited up to total coverage Θ, and it enters the layers at height n. Therefore, J_n necessarily depends on the height i.e. on the number of layers n of the structure (compare e.g. with [2, 3]).

The rate equations describing the time evolution of coverage θ_n of a given layer n are obtained by considering the effective mass currents affecting the growth. The adatom flux on terrace n is simply given by two terms: the adatom flux $J_n(\theta_{n-1} - \theta_n)$ from the wetting layer on the terrace, and the redistribution current from upper layers. The redistribution current, on the other hand, is given by the product of three factors: (1) number of adatoms $\sum_{k=n+1}^{N_{\mathrm{top}}} J_k(\theta_{k-1} - \theta_k)$ entering layers above the nth level, (2) the uncovered area $\theta_{n-1} - \theta_n$ on nth terrace, and (3) the coefficient γ_n, which describes the diffusion of mass to the nth layer from layers above it. The total flux of adatoms entering into the layer n is then given by $J_+(n) = (\theta_{n-1} - \theta_n)[J_n + \gamma_n [\sum_{k=n+1}^{N_{\mathrm{top}}} J_k(\theta_{k-1} - \theta_k)]]$. In this expression J_n is the contribution from the feeding current and in the redistribution part γ_n has the role of transfer rate for crossing the nth step edge. The decrease of the coverage of the nth level is similarly given by (1) the product of the adatom flux $J_n(\theta_{n-1} - \theta_n)$ on the nth terrace, (2) the available uncovered area $1 - \theta_{n-1}$ below it and (3) the rate coefficient γ_{n-1} describing the diffusion from the nth layer to the layers below (i.e. the rate for crossing the $(n-1)$th step edge), resulting in $J_-(n) = \gamma_{n-1} J_n(\theta_{n-1} - \theta_n)(1 - \theta_{n-1})$. The total rate of change of the coverage is now given by $\mathrm{d}\theta_n/\mathrm{d}t = J_+(n) - J_-(n)$. Finally, by collecting all terms together and rearranging them, the rate equations read

$$\frac{\mathrm{d}}{\mathrm{d}t}\theta_n = J_n(\theta_{n-1} - \theta_n)[1 + \gamma_n\theta_n + \gamma_{n-1}\theta_{n-1} + \Delta_n], \qquad (2)$$

where the effects due to the dependence of adatom feeding current J_n on the structure morphology are now taken into account by the term

$$\Delta_n = \frac{\gamma_n}{J_n}\sum_{k=n}^{N_{\mathrm{top}}} \theta_k(J_k - J_{k+1}) - \gamma_{n-1}. \qquad (3)$$

The rates γ_n need to be normalized so that $0 \leqslant \gamma_n \leqslant 1$, in order to take care so that $0 \leqslant \gamma_n\theta_n \leqslant 1$ for all n in equation (2), thus ensuring mass conservation in the redistribution of adatoms. Without the term Δ_n the rate equations (2) are similar to the set of equations given by Fu and Wagner [22, 23]. It should be noted that the physical origin of this additional term lies in the structure height dependence of the feeding current. When $J_n \to J_0$ for all n also $\Delta_n \to 0$, leading immediately to a similar set of equations as in [22, 23]. When $\gamma_n \to \gamma_0 = f$ for all n with $0 < f < 1$, the model is completely similar to the DCSM model in [22].

2.2. The interlayer mass transfer rate

The definition of interlayer mass transfer rate γ_n and its relation to the surface energetics given by equation (1) requires some closer discussion. In the case of Pb/Cu(111) and Pb/Si(111) the interlayer mass transfer originates from the microscopic atomic transitions downwards from the upper to lower terraces as discussed in [2, 3, 13, 17, 18]. First, we note that in inferring the parametrization of the Friedel model from the experimental

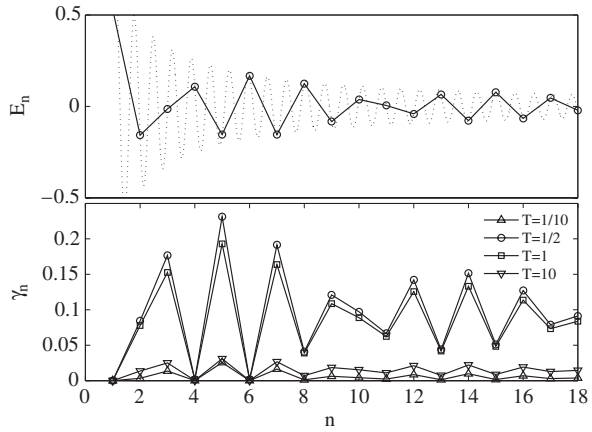

Figure 1. Surface energy E_n as described by the Friedel model (upper panel) and corresponding rate coefficients γ_n at different temperatures (lower panel). The beating behaviour (solid line) originates from the oscillations in the Friedel model (dotted line) when energy is calculated for integer values of n. In all cases, dimensionless energy $E_n \to E_n/A$ and temperature $T \to k_\mathrm{B}T/A$ are used.

results, it has been assumed that the equilibrium distribution of structures with certain heights are related to the Boltzmann distribution $p_n \propto \exp[E_n/k_\mathrm{B}T]$ [5, 6]. Secondly, we assume that in the nonequilibrium case the transition rates for the atomistic step crossings g_n fulfil the condition of detailed balance $p_{n+1}g_n = p_n g_{n-1}$. Therefore, we can choose g_n to follow the Arrhenius-type relation $g_n = \exp[-E_n/k_\mathrm{B}T]$ in agreement with detailed balance. In defining the mass transfer coefficient $\gamma_n \propto g_n$ to be used in the model given by equations (2) and (3) one needs to ensure the mass conservation so that $0 \leqslant \gamma_n \leqslant 1$. A definition for mass transfer rate which is consistent with these assumptions is given by

$$\gamma_n = \frac{g_n - \min[g_n]}{\max[g_n]}, \qquad g_n = \exp[-E_n/k_\mathrm{B}T]. \tag{4}$$

The relation of the rate coefficients γ_n to the Friedel oscillations for complete layers (n integer) is shown in figure 1. The beating behaviour of the Friedel oscillations now becomes reflected also in the mass transfer rate γ_n, and this arises simply from the fact that energy barriers are calculated only for complete layers corresponding to integer values of n. The alternating stability of the layers comes now through the rate γ_n and is therefore a built-in feature of the model. It is essential to keep in mind that the energetic stability itself is not the prediction of the model, but the model shows how the energetic stability affects the morphology. At high and low temperatures the oscillations become heavily damped and $\gamma_n \to \gamma_0 = 0$. In this limit the DSCM and simultaneous multilayer growth are recovered (to be compared with case $f = 0$ in [22]).

2.3. The feeding current

The adatoms feeding the growth of the different layers, i.e. the feeding current, come from the pre-deposited wetting layer of adatoms, which covers the surface of the substrate and has total coverage Θ, typically 5–12 monolayers [2, 3]. In order to specify the generic form of the feeding current, we make an assumption that the current from a given layer to the next one depends on the current entering into layers below it. Moreover, the adatoms may either take all step lengths from 1 to n when entering the layer n, or otherwise single step jumps with a broad distribution of waiting times between jumps. These alternatives lead us to consider a random process, where the crossing of a layer is a rare event, either with a broad distribution of jump lengths $n^{-(1+\beta)}$ or waiting times $\tau^{-(1+\beta)}$ with $0 < \beta \leqslant 2$ [24]. The cumulative probability $P(n)$ to enter the layer n can be approximated in the continuum limit to be $P(n) \propto \int n'^{-(1+\beta)}\mathrm{d}n' \propto n^{-\beta}$. Therefore, the feeding current $J_n \propto P(n)$ can be assumed to have a form

$$J_n = J_0\, n^{-\beta}, \qquad 0 < \beta \leqslant 2. \tag{5}$$

The factor J_0 can adjusted so that the total amount of mass in the final structures is equal to the pre-deposited amount Θ of material by requiring that $\Theta = \sum_n J_n$. In practice we use Θ as a parameter and show the resulting structures as a function of increasing Θ. Therefore, results have significance up to the given pre-deposited amount of material. It should be noted, however, that in a real situation not all pre-deposited mass is consumed by the growing structures, but in order to reach structures with n layers pre-deposition of $\Theta > n$ is required.

It can be noted that the value $\beta \to 0$ corresponds to the 'ballistic' transport with feeding current becoming constant, while the other limit $\beta = 2$ corresponds to the 'diffusive' or ordinary random walk (for details, see e.g. [24]). Of course, the notions 'ballistic' and 'diffusive' refer to a random walk with a large number of repeated jumps or a large number of layers (see the standard derivations e.g. in [24]), and are not meant to be taken literally in the present situation but only as a convenient way to refer to the essential qualitative differences of the adatom feeding process. In what follows we concentrate on cases $1/2 \leqslant \beta < 2$, because firstly, adatom current with equal transition probability for all heights (i.e. ballistic) is implausible and would require very special conditions, and secondly, by choosing $\beta \geqslant 2$, results similar to $\beta = 2$ are expected, because then the transport is slow enough so that additional slowing down does not affect the outcome of growth. As will be seen, in region $1/2 < \beta < 1$ there is a gradual change from slightly rounded tower-like structures to nearly perfect ones, while with $\beta > 1$ the exact values of β have no further consequences on the morphology.

2.4. The nucleation of new layers

The new layers are formed on top of the existing layers if there is a large enough stable nucleus available to support the further growth. Thus the formation of this nucleus is crucial for the growth of the nanotowers; the growth of layers is prohibited if no stable nuclei are formed. The probability of forming a stable nucleus depends on the critical size of the terrace needed for two adatoms to merge. The nucleation rate ω for this process can be calculated within the 'lonely adatom model' (LAM) [19, 20], where two isolated adatoms on a terrace meet and form immediately a stable nucleus. The probability of nucleation depends only on the adatom flux and

residence time on an island with radius R. The residence time, on the other hand, is related to the energy barrier needed to overcome the descending terrace edge. According to the LAM, the nucleation rate is obtained in form [20]

$$\omega_n = \frac{\pi^2 J_n^2 R^5}{2\gamma_{n-1}}. \tag{6}$$

In defining the relation of ω_n to the critical radius R_n^c needed for nucleation of the new layer, we follow the LAM in requiring that nucleation takes place when the probability that no nucleation has occurred is equal to $1/2$ (see [20] for derivation), resulting in $R_n^c = (7\ln 2/\pi^2)^{1/5}(\gamma_{n-1}/J_n)^{1/5}$. When the radius of the topmost layer reaches the critical radius R_n^c a new layer can nucleate on it. In practice this is done by multiplying the terms responsible for the nucleation of a new, nth layer in equation (2) with a Heaviside step function $\mathrm{H}(\theta_{n-1} - \theta_{n-1}^c)$, where $\theta_n^c = \pi(R_n^c)^2$ is the critical coverage needed for nucleation. Formally, this means replacing term $J_n[\theta_{n-1} - \theta_n]$ with $J_n[\theta_{n-1} - \theta_n]\mathrm{H}(\theta_{n-1} - \theta_{n-1}^c)$ in equation (2) to prevent the premature formation of new layers.

2.5. Measures to monitor morphology

Finally, in order to make the essential features of the growth visible and examinable, we need suitable measures to monitor the time evolution of the morphology of nanostructures or nanostructured layers. Such measures, which are also experimentally accessible, are most often based on measurements of the partial surface coverages. However, the coverages alone are not yet very convenient quantities for monitoring the growth and stability of layers and the evolution of the structure morphology. Instead, a better measure for indicating the evolution of morphology can be based on the statistical roughness or RMS height fluctuations of the structures defined as [20]

$$W = \left[\sum_{k=0}^{\infty}(k - \Theta)^2\varphi_k\right]^{1/2}, \tag{7}$$

where $\Theta = \sum_{k=1}^{\infty}\theta_k$ and $\varphi_k = \theta_{k-1} - \theta_k$. Because φ_n can be interpreted as the probability that an arbitrary point on the structure is on layer n, it can taken as the probability distribution of the local height [19, 20]. Thus the RMS height fluctuations from the mean Θ define the effective roughness of the structure and directly give information of the morphology of the structures. For a simple simultaneous multilayer growth leading to the formation of mounds or tipped mounds [19, 20], the roughness has a simple power law behaviour $W = \sqrt{\Theta}$, revealing a scaling property of the cluster structures. For the simultaneous bilayer type growth leading to the formation of nanotowers, the roughness is expected to be an oscillating function with deep minima at the locations of the stable towers.

3. Results

The time evolution of the nanostructure morphology is obtained by solving equation (2) numerically for different temperatures and parameters β. With different choice of parameters the model describes different nanostructure morphologies, which are also clearly indicated by the behaviour of roughness W. In representing the results, we have chosen to use the total coverage Θ as a parameter, but in practice, the value of Θ is set by the initial condition of a pre-deposited number of layers. In all cases, we assume that all pre-deposited material is available for growth.

An example of the evolution of the nanotower morphology is shown in figure 2 for $T = 1$ (corresponding to temperatures 150–250 K for Pb/Si and 300–500 K in Pb/Cu depending on the exact parametrization) and for $\beta = 1/2$ and 1. In this case, nanotowers with heights 4, 6, 8 and 11, 13 and 15 (and also 17 although not shown in figure 2) are clearly tower-like structures. These sizes correspond to the deep crevices in W, and when they are obtained, the growth is retarded. It should be noted that the time in the calculations depends on the parameter values and its absolute scale cannot be fixed without further knowledge of the absolute values of J_n and g_n. Nevertheless, relative time differences are meaningful. This allows us to conclude that in figure 2, where coverages θ_n are shown as a function of time, the growth is seen to take place so that two layers grow nearly simultaneously but between these periods there is a period of retardation or slowing down of growth. With increasing β, the retardation period increases. In fact, when $\beta \to 2$, the growth practically stops at stable heights, but morphology remains the same as for $\beta = 1$ when the structures are already nearly perfect towers. By comparing the cases $\beta = 1/2$ and 1 in figure 2, it is seen that the variations in β do not affect much the morphology of the towers with stable heights. This situation holds in practice for all values of $\beta > 1/2$, and therefore β controls mainly the time evolution of the structures without affecting too much the height selection and morphology. When $\beta \ll 1/2$ the structures will become more rounded, and eventually in the limit $\beta \to 0$ they resemble structures shown in figure 3 at high and low temperatures. Therefore, certain reduction of the feeding current with increasing height is needed, but the exact value of β is not crucial.

The model results are compared in table 1 with experimental results for Pb/Cu and Pb/Si systems. As is seen from this comparison, the stability of heights 6 and 8 as well as 15 and 17 are quite a robust outcome both in model calculations and in experiments. It is of interest to note that in our model, the height 4 appears but it is not observed in experiments [2–6, 8–11]. Moreover, the height 10 seen in some experiments is missing in our model, which is probably due to the fact that this height occurs near the beating regions of the surface energy (see figure 1). Also, heights 12 and 14 reported in some Pb/Si systems seem to depend very delicately on the energetics. In general, very small changes in the energetics may change considerably the behaviour near beating regions, which explains the ambiguity of the results for the stability of heights 4, 10, 12 and 14.

The effect of ambient temperature on growth is expected to be significant in determining the stable heights. This is demonstrated in figure 3 where three temperatures $T = 1/10$, $1/2$ and 10 are compared with case $T = 1$ in figure 2.

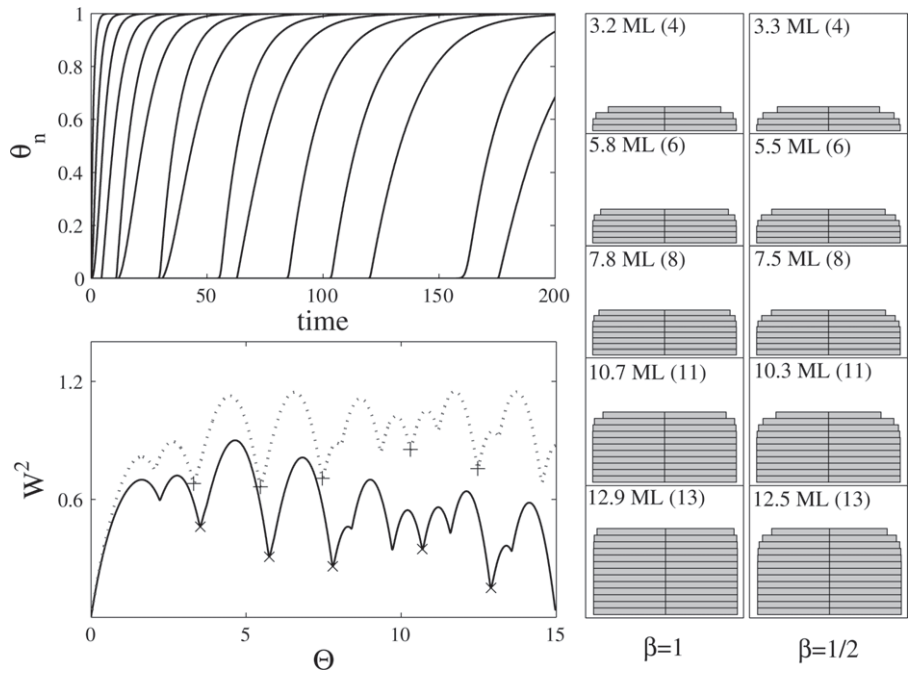

Figure 2. Nanotower growth and the evolution of partial coverages of different layers θ_n and the roughness W^2 for $T = 1$ and $\beta = 1$ (solid line) and for $\beta = 1/2$ (dotted line). Nanotower morphologies at positions of roughness minima as indicated are shown in the panel on the right. Also the total coverage and the number of completed layers are given.

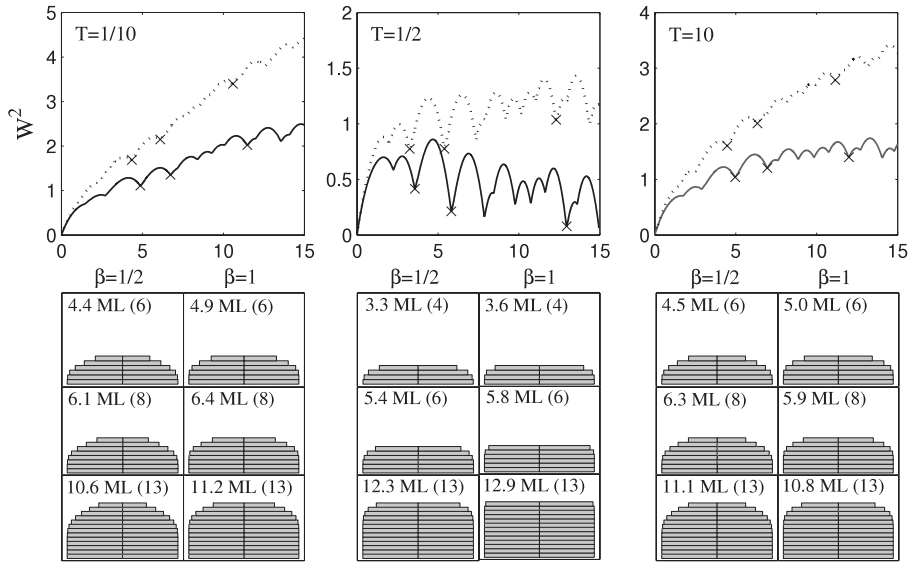

Figure 3. Temperature effect on nanotower growth as monitored through the roughness W^2. Parameters are $T = 1/10$, $1/2$ and 10 and $\beta = 1$ (solid line) and $1/2$ (dotted line). Note the similarity of results for low ($T = 1/10$) and high ($T = 10$) temperatures, and the resulting mound-like morphology.

Table 1. Model results for stable heights of nanotowers compared with experimental results. Note that in some references the counting of layers/steps is done differently (compare e.g [2, 7] to [8, 4–6]). In the table counting based on complete layers is used.

Ref.	Stable heights										System	Temp. (K)
Model	4	6	8	—	11	—	13	—	15	17	Pb/Cu(Si)	90(180)–350(700)
[8]	—	6	8	—	11	—	—	—	15	17	Pb/Cu	300–400
[7]	—	6	8	10	—	12	—	14	15	17	Pb/Si	150–250
[4, 5]	—	6	8	10	—	12	13	—	15	17	Pb/Si	150–280

The corresponding rates γ_n based on the Friedel model are shown in figure 1. From the results in figure 3 it can be seen that at low temperatures only heights 6 and 8 are nanotower-like and for larger structures the morphology rapidly turns to mounds or rounded huts, reminiscent of 'wedding-cake' structures [19, 20] and Poissonian growth with $W \propto \sqrt{\Theta}$. In these limiting regions the layer dependent oscillations in the interlayer mass transfer coefficient γ_n become vanishingly small and $\gamma_n \to 0$. In this region simultaneous multilayer growth as described by DCSM is retained.

In summary, the results show that at intermediate temperatures $1/2 < T < 2$ there is a temperature window, where even heights are stable up to height 8, and after that the odd heights from 11 onwards become more stable than the even heights. The temperature window where stable structures are obtained corresponds to real temperatures of about 90 K $< T <$ 350 K for Pb/Si ($A = 150$ meV) and about 180 K $< T <$ 700 K for Pb/Cu ($A = 300$ meV). This temperature window is in reasonably good agreement with experimental observations, where stable structures in Pb/Si systems have been reported in the temperature windows 150–280 K [2–6] and 250–400 K in Pb/Cu [8–11].

4. Conclusions

It is shown here that a simple phenomenological model, which describes the time evolution of wedding-cake type structures, reproduces the typical morphologies of Pb nanotowers as they are observed in heteroepitaxy on Si(111) and Cu(111) surfaces. The results show that the morphological evolution of such structures is simply related to the macroscopic mass currents that originate from the feeding of adatoms from the wetting layer and the adatom redistribution due to interlayer transitions governed by Friedel-type oscillating energetics. These simple conditions appear to be enough to describe the growth of nanotowers. Notable is the clear simultaneous bilayer growth, as indicated by the grouping of coverages in groups of two and the accompanying double peaked oscillations of roughness. This feature of bilayer growth is also observed in experiments [2, 3, 8, 9]. Moreover, the temperature dependence of nanotower morphologies and the temperature window, where such structures are obtained, are correctly described by the phenomenological model presented here.

These notions about the basic phenomenology of growth and the basic processes behind it are in qualitative agreement with experimental observations of the growth of nanotowers on Pb/Cu(111) and Pb/Si(111). Therefore, the present model suggests that such morphologies are rather robust outcomes of growth and are expected whenever the basic phenomenological conditions of oscillating energetics, feeding current diminishing with increasing structure height and the conditions of critical size for nucleation of new layers are fulfilled.

Acknowledgment

This work has been supported by the Academy of Finland through grant SA 1210516.

References

[1] Luh D-A, Miller T, Paggel J J, Chou M Y and Chiang T-C 2001 *Science* **292** 1131
[2] Hupalo M and Tringides M C 2002 *Phys. Rev.* B **65** 115406
[3] Menzel A, Kammler M, Conrad E H, Yeh V, Hupalo M and Tringides M C 2003 *Phys. Rev.* B **67** 165314
[4] Czoschke P, Hong H, Basile L and Chiang T-C 2003 *Phys. Rev. Lett.* **91** 226801
[5] Czoschke P, Hong H, Basile L and Chiang T-C 2004 *Phys. Rev. Lett.* **93** 03603
[6] Czoschke P, Hong H, Basile L and Chiang T-C 2005 *Phys. Rev.* B **72** 075402
[7] Özer M M, Jia Y, Wu B, Zhang Z and Weitering H H 2005 *Phys. Rev.* B **72** 113409
[8] Otero R, Vázquez de Parga A L and Miranda R 2002 *Phys. Rev.* B **66** 115401
[9] Ogando E, Zabala N, Chulkov E N and Puska M J 2004 *Phys. Rev.* B **69** 153410
[10] Ogando E, Zabala N, Chulkov E N and Puska M J 2005 *Phys. Rev.* B **71** 205401
[11] Calleja F, Passeggi M C G, Hinarejos J J, Vásquez de Parga A L and Miranda R 2006 *Phys. Rev. Lett.* **97** 186104
[12] Wei C M and Chou M Y 2002 *Phys. Rev.* B **66** 233408
[13] Upton M H, Wei C M, Chou M Y, Miller T and Chiang T-C 2004 *Phys. Rev. Lett.* **93** 026802
[14] Jeong H-C and Williams E D 1999 *Surf. Sci. Rep.* **34** 171
[15] Israeli N and Kandel D 1999 *Phys. Rev.* B **60** 5946
[16] Degawa M, Thürmer K and Williams E D 2006 *Phys. Rev.* B **74** 155432
[17] Morgenstern K, Laegsgaard E and Besenbacher F 2005 *Phys. Rev. Lett.* **94** 166104
[18] Jeffrey C A, Conrad E H, Feng R, Hupalo M, Kim C, Ryan P J, Miceli P F and Tringides M 2006 *Phys. Rev. Lett.* **96** 106105
[19] Krug J, Politi P and Michely T 2000 *Phys. Rev.* B **61** 14037
[20] Krug J 2002 *Physica* A **313** 47
[21] Voigtländer B and Weber T 1996 *Phys. Rev.* B **54** 7709
[22] Fu Q and Wagner T 2003 *Phys. Rev. Lett.* **90** 106105
[23] Fu Q and Wagner T 2005 *Appl. Surf. Sci.* **240** 189
[24] Weiss G H 1994 *Aspects and Applications of the Random Walk* (Amsterdam: North-Holland)